


Facile synthesis of some 5-(3-substituted-thiophene)-pyrimidine derivatives and their pharmacological and computational studies

S.H. Sukanya ^a, Talavara Venkatesh ^{a*} , S.J. Aditya Rao ^b, N. Shivakumara ^c, Muthipeedika Nibin Joy ^d

- a: Department of P.G. Studies and Research in Chemistry, Jnanasahyadri, Kuvempu University, Shankaraghatta 577451, Karnataka, India
b: Plant Cell Biotechnology Department, CSIR-Central Food Technological Research Institute, Mysore 570020, Karnataka, India
c: Department of Chemistry, Ramaiah Institute of Technology, Bangalore 560054, India
d: Innovation Center for Chemical and Pharmaceutical Technologies, Institute of Chemical Technology, Ural Federal University, 19 Mira St., Yekaterinburg 620002, Russia
* Corresponding author: venkateshatalwar@gmail.com

This article belongs to the regular issue.

© 2021, The Authors. This article is published in open access form under the terms and conditions of the Creative Commons Attribution (CC BY) license (<http://creativecommons.org/licenses/by/4.0/>).



Abstract

A series of 5-(3-substituted-thiophene)-pyrimidine derivatives (**3a-d**) were synthesized *via* Knoevenagel condensation reaction in aqueous ethanol using H₂O₂:HCl as a catalyst. Their pharmacological effects were evaluated. Analytical and spectroscopic methods confirmed the structures of the target molecules. The antibacterial activity studies revealed that compounds **3b** and **3d** exhibited the most effective zone of inhibition against bacterial strains *E. coli* and *S. aureus*, respectively. The *in vitro* cytotoxicity was carried out by MTT assay against MCF-7 cell line. The results showed the excellent selectivity for all four compounds, among which the compound **3a** exhibited remarkable cytotoxicity with a minimum cell viability range of 23.68 to 44.16%. The interaction of compounds with calf thymus DNA was determined using UV-absorption spectroscopy. The results confirmed that all the synthesized compounds interacted strongly with CT DNA through electrostatic or groove binding. *In silico* ADME-toxicology studies indicated that all the molecules under investigation are non-toxic with good oral bioavailability. The drug-likeness score indicated that they are suitable as drug-leads. *In silico* molecular docking the specified compound **3b** binds with GlcN-6-P and P38 MAPk with a minimum binding energy of -7.9 and -6.4 kcal/mol, respectively. DFT study demonstrated that the compound **3d** was chemically and biologically more reactive due to less energy gap.

Keywords

biological studies
DNA binding
ADME-toxicology study
SAR study
molecular docking and DFT studies

Received: 02.09.2021

Revised: 11.10.2021

Accepted: 12.10.2021

Available online: 15.10.2021

1. Introduction

Heterocyclic compounds play a predominant role in medicinal chemistry and synthetic organic chemistry due to their massive biological importance. The synthesis of nitrogen and sulphur containing fused heterocyclic compounds with multi-structures in one molecule has attracted the attention of medicinal chemists and researchers due to their multifaceted pharmacological activities [1-2]. Among them, pyrimidine and thiophene have been recognized as key scaffolds owing to their important biological

significances and interesting therapeutic properties including anti-tubercular [3], anticancer [4], anti-HIV [5], antibacterial [6], antifungal [7], antitumor [8], also used as potent EGFR inhibitor [9, 10], protein kinase inhibitors [11-14] and 5-HT₇ receptors [15].

Moreover, the heterocyclic compounds increase the strength of the molecules by forming hydrogen bonds with DNA. Hence, the interactive study of heterocyclic moieties with DNA is essential for estimating their anticancer activity and elucidates the viable mechanism of their action. Therefore, DNA binding is considered as an essential ex-

perimental step to measure anticancer drugs activity because most anticancer drugs specifically target the DNA [16]. Heterocyclic compounds appear to be most effective against various cancers. Around 60% of the medicines used for cancer treatment are based on heterocyclic moieties. Among the various heterocyclic moieties, nitrogen and sulphur-based compounds are effective against different types of cancers [17–19].

Cancer is a group of diseases in which the abnormal cells grow uncontrollably by disregarding the normal rules of cell division. Cancer is caused by many external (tobacco, chemicals, radiation and infectious organisms) as well as some internal factors (inherited mutations, hormones, immune conditions and random mutations). There are different types of cancer such as breast cancer, bladder cancer, kidney cancer, leukaemia, liver cancer, lung cancer, melanoma, pancreatic cancer, prostate cancer, thyroid cancer etc. [20]. The breast cancer is one of the most frequently diagnosed cancers and the leading cause of death in females worldwide, with more than 1.5 million new cases recorded every year. It is also the fifth-highest cause of death in the world [21]. The modern methods of chemotherapy suffer from the main disadvantages: side effects and drug resistance. Therefore, continued search for novel and safer anticancer drugs remains essential [22].

Pollution is one of the critical problems that the synthetic organic chemist faces in designing the organic reactions for the synthesis of pharmacologically active compounds. Thus, development of an environmentally-friendly chemical process that induces necessary organic transformation is one of the most important goal of sustainable progression [23]. Therefore, "green chemistry" becomes a promising approach that meets the requirements of the chemical and pharmaceutical industries. The replacement of hazardous solvents with eco-friendly solvents is an acceptable and valuable approach in a chemical reaction. Hence, the use of a hypochlorous acid (HOCl) as a green halogenating agent [24] is highly advantageous over other catalysts, including cost-effectiveness, efficiency and readily availability. Earlier, our research group has reported the synthesis of different pyrimidine derivatives and other biologically important heterocyclic compounds [25–27]. Some of the drugs containing pyrimidine nucleus available in the market are depicted below (Fig. 1).

Based on the above findings, we herein report the application of H₂O₂:HCl as a green halogenating catalyst for the synthesis of 5-(3-substituted-thiophene)-pyrimidine derivatives of considerable pharmacological relevance.

2. Experimental

2.1. Materials and Method

All chemicals and calf thymus DNA were purchased from Aldrich Chemical Company, and the reaction was performed at refluxed condition and solvents were used without further purification. Analytical TLC was performed with E. Merck silica gel GF254 glass plates. Visualization of the developed

chromatogram was performed by UV light (254 and 356 nm). The melting points of the products were determined in open capillary tubes and uncorrected. The ATR-IR spectra were obtained using Bruker FTIR Alpha spectrometer. The ¹H NMR and ¹³C NMR spectra were recorded on Bruker 400 MHz and 100 MHz in DMSO-d₆ as a solvent. Mass spectra were obtained by Agilent 1200 series LC and Micromass Q spectrometer. The DNA binding studies were carried on Elico SL 159 UV-Visible spectrophotometer in 200–500 nm range equipped with 1.0 cm quartz cell at room temperature. The anticancer activity was carried out in the Department of Microbiology, Maratha Mandal's NGH Institute of Dental Sciences and Research Centre, Belgaum, Karnataka. The computational studies were carried out by Density functional theory (DFT)/B3LYP method using Gaussian 09 software using 6-31G (d, p) basis set at gaseous phase.

2.2. General procedure for the synthesis of 5-(3-substituted-thiophene)-pyrimidine derivatives (3a-d)

The synthesis of 5-(3-substituted-thiophene)-pyrimidine derivatives (3a-d) were carried out by the reaction of barbituric/thiobarbituric acid (1, 1mmol) with 3-substituted-thiophene-2-carboxaldehyde (2, 1mmol) in the presence of 15 mL aqueous ethanol using 6% H₂O₂:HCl (2:1) as a catalyst. The reaction mixture was refluxed at 80 °C for about 10–15 min and the progress of the reaction was monitored by TLC (Ethyl acetate and Petroleum ether). After the completion of the reaction, the reaction mixture was cooled to room temperature and poured into the 100 mL flake ice with vigorous stirring to get solid precipitated out. The crude mixture was filtered, washed and recrystallized with absolute ethanol to afford pure solid products.

2.2.1. 5-(Thiophen-2-ylmethylidene)pyrimidine-2,4,6(1H,3H,5H)-trione (3a)

Yield: 96%, Yellow solid; MP: 280–282 °C. IR (ATR, ν cm⁻¹): 3373 (NH), 1654 (C=O), 1529 (C=C). ¹H NMR (400 MHz, DMSO-d₆, δ ppm): 7.31–7.33 (t, *J*= 8 Hz, 1H, Ar-H), 8.13–8.24 (m, 2H, Ar-H), 8.53 (s, 1H, CH), 11.17 (s, 1H, NH), 11.21 (s, 1H, NH). ¹³C NMR (100 MHz, DMSO-d₆, δ ppm): 112.035, 128.808, 136.776, 142.526, 146.116, 146.291, 150.679, 163.453 and 163.950 (C=O). HRMS: *m/z* 221.9054 [M+H]⁺. Anal. Calcd for C₉H₆N₂O₃S: C 48.64, H 2.72 and N 12.61%. Found: C 48.59, H 2.68 and N 12.53%.

2.2.2. 5-[(3-Methylthiophen-2-yl)methylidene]pyrimidine-2,4,6(1H,3H,5H)-trione (3b)

Yield: 94%, Yellow solid; MP: 302–306 °C. IR (ATR, ν cm⁻¹): 3225 (NH), 2858 (CH₃), 1703 (C=O), 1542 (C=C). ¹H NMR (400 MHz, DMSO-d₆, δ ppm): 2.24 (s, 3H, CH₃), 7.21–7.23 (d, *J*= 8 Hz, 1H, Ar-H), 8.16–8.18 (d, *J*= 8 Hz, 1H, Ar-H), 8.53 (s, 1H, CH), 11.17 (s, 1H, NH), 11.24 (s, 1H, NH). ¹³C NMR (100 MHz, DMSO-d₆, δ ppm): 19.922 (CH₃), 114.870, 135.252, 136.011, 145.166, 147.180, 154.915, 158.106, 167.728 and 168.497 (C=O). HRMS: *m/z* 235.9774 [M+H]⁺. Anal. Calcd for C₁₀H₈N₂O₃S: C 50.84, H 3.41 and N 11.86%. Found: C 50.79, H 3.36 and N 11.80%.

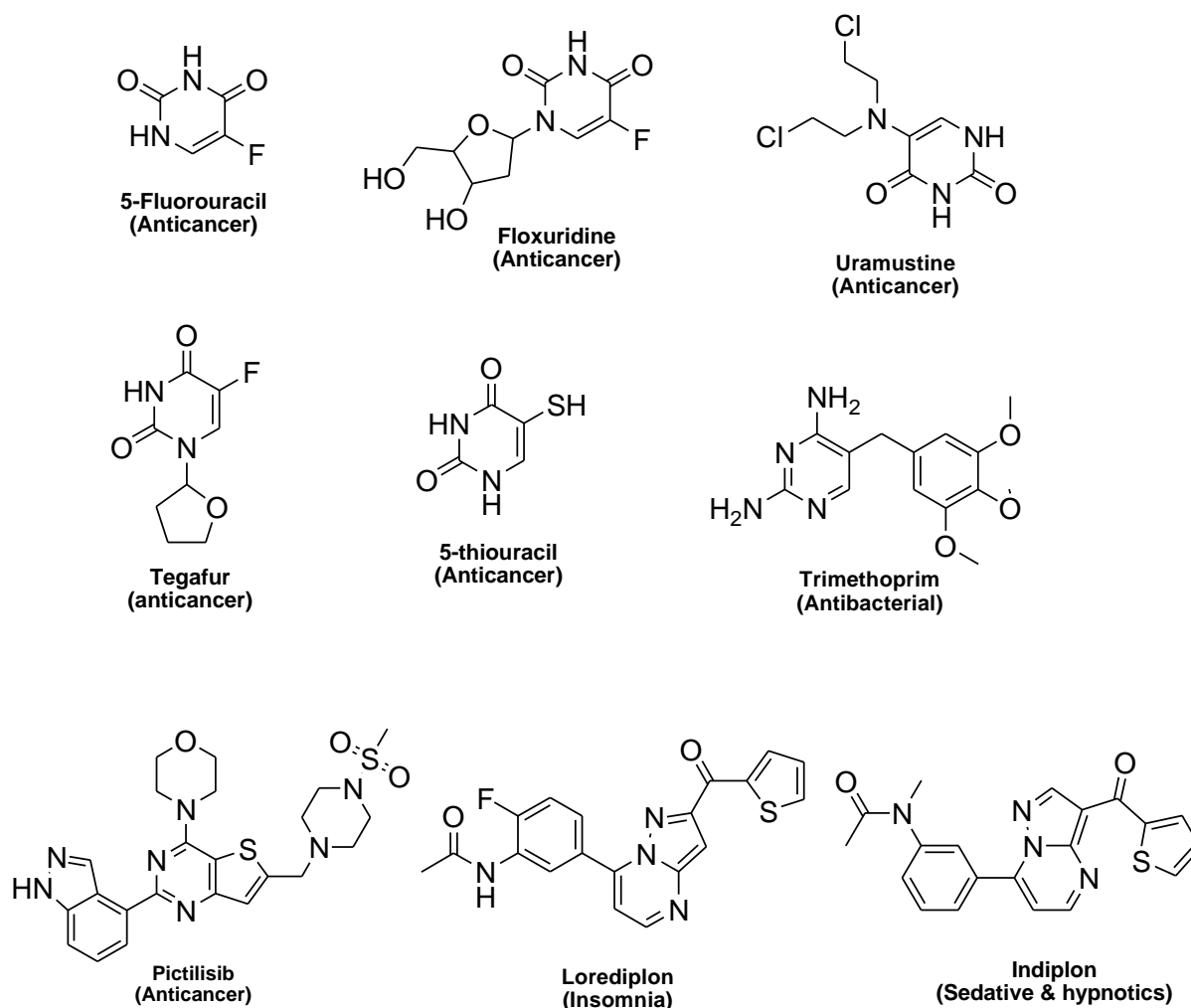


Fig. 1 Some of the drugs containing pyrimidine nucleus available in the market

2.2.3. 5-(Thiophen-2-ylmethylidene)-2-thioxodihydropyrimidine-4,6(1H,5H)-dione (3c)

Yield: 93%, Green solid; MP: 320–322 °C. IR (ATR, ν cm⁻¹): 3106 (NH), 1760 (C=O), 1559 (C=C), 1156 (C=S). ¹H NMR (400 MHz, DMSO-d₆, δ ppm): 6.86–6.88 (d, J = 8 Hz, 1H, Ar-H), 8.20 (s, 1H, CH), 8.34–8.36 (d, J = 8 Hz, 2H, Ar-H), 12.20 (s, 1H, NH), 12.30 (s, 1H, NH). ¹³C NMR (100 MHz, DMSO-d₆, δ ppm): 114.713, 116.139, 124.434, 139.254, 157.012, 160.480, 162.825, 164.168 (C=O) and 178.617 (C=S). HRMS: m/z 237.9467 [M+H]⁺. Anal. Calcd for C₉H₆N₂O₂S₂: C 45.36, H 2.54 and N 11.76%. Found: C 45.30, H 2.49 and N 11.71%.

2.2.4. 5-[(3-Methylthiophen-2-yl)methylidene]-2-thioxodihydropyrimidine-4,6(1H,5H)-dione (3d)

Yield: 95%, Green solid; MP: 310–312 °C. IR (ATR, ν cm⁻¹): 3108 (NH), 2852 (CH₃), 1704 (C=O), 1516 (C=C), 1200 (C=S). ¹H NMR (400 MHz, DMSO-d₆, δ ppm): 2.24 (s, 3H, CH₃), 7.22–7.24 (d, J = 8 Hz, 1H, Ar-H), 8.17–8.19 (d, J = 8 Hz, 1H, Ar-H), 8.54 (s, 1H, CH), 11.18 (s, 1H, NH), 11.25 (s, 1H, NH). ¹³C NMR (100 MHz, DMSO-d₆, δ ppm): 26.806 (CH₃), 114.280, 128.031, 128.903, 129.867, 130.391, 130.892, 142.472, 163.552 (C=O) and 173.358 (C=S). HRMS: m/z 251.9608 [M+H]⁺. Anal. Calcd for

C₁₀H₈N₂O₂S₂: C 47.60, H 3.20 and N 11.10%. Found: C 47.55, H 3.16 and N 11.06%.

2.3. Pharmacological studies

2.3.1. Antibacterial activity

Antibacterial activity of the synthesized compounds (3a-d) was carried out by the agar well diffusion method [28] using two bacterial strains (Gram-negative and Gram-positive) *Escherichia coli* (MTCC-1559) and *Staphylococcus aureus* (MTCC-902). DMSO was used as negative control and Ciprofloxacin as standard drug. The test compounds were dissolved in DMSO at two different concentrations, 20 and 40 μ g/mL.

2.3.2. Cytotoxicity

In vitro cytotoxicity was assessed by the MTT assay method [29] against MCF-7 (Breast cancer) cell line. The cells were seeded in a 96-well flat-bottom microplate and maintained at 37 °C in 95% humidity and 5% CO₂ overnight. Different concentration (200, 100, 50, 25, 12.5 and 6.25 μ g/mL) of samples were treated. The cells were incubated for another 48 h, and the wells were washed twice with PBS. 20 μ L of the MTT staining solution was added to each well, and the plate was incubated at 37 °C for 4 h. The medium with MTT was discarded, and 100 μ L of

DMSO was added to each well to dissolve the formazan crystals. The absorbance was recorded at 570 nm using a microplate reader. The percentage of cell survival was calculated by using the following formula:

$$\% \text{ of cell survival} = \frac{\text{Mean O. D. of test compound}}{\text{Mean O. D. of Negative control}} \cdot 100. \quad (1)$$

2.3.3. DNA binding study

DNA binding study was assessed by using electronic spectroscopy. A solution of CT DNA in 50 mM Tris-HCl/50 mM NaCl buffer solution was prepared at pH 6.9–7.01. In buffer solution, the ratio of absorption values of CT DNA at 260 and 280 nm is 1.8–1.9, indicating that DNA was free of proteins [30]. Then a concentrated stock solution of DNA was prepared in 50 mM Tris-HCl, 50 mM NaCl in double distilled water at pH 6.9–7.01. The concentration of CT DNA was determined per nucleotide by taking the absorption coefficient ($6600 \text{ dm}^3 \text{ mol}^{-1} \text{ cm}^{-1}$) at 260 nm [31]. Stock solutions were stored at 4 °C. 2 mL of the solution was taken containing a fixed concentration of the compounds (**3a-d**) with CT DNA (0 to 350 μL of a $0.5025\text{--}6.0670 \cdot 10^{-7}$ M stock CT DNA solution). A blank solution containing the same concentration of DNA was used as a reference. Solutions were prepared by mixing the compound and CT DNA in DMSO medium and then recording the UV absorption spectra by adding 25 to 350 μL DNA to the compound. The spectra were recorded against a blank solution containing the same concentration of DNA ($4.0909 \cdot 10^{-6} \text{ mol L}^{-1}$). The intrinsic binding constant K_b was obtained by using the following equation [32]:

$$\frac{[\text{DNA}]}{(\epsilon_A - \epsilon_B)} = \frac{[\text{DNA}]}{(\epsilon_B - \epsilon_F)} + \frac{1}{K_b(\epsilon_B - \epsilon_F)}, \quad (2)$$

where, ϵ_A , ϵ_B and ϵ_F corresponds to the apparent, bound and free compound extinction coefficients, respectively. A plot of $\frac{[\text{DNA}]}{(\epsilon_A - \epsilon_F)}$ versus $[\text{DNA}]$ gave a slope of $\frac{1}{(\epsilon_B - \epsilon_F)}$ and Y-intercept equal to $\frac{1}{K_b(\epsilon_B - \epsilon_F)}$. Hence K_b is the ratio of slope to intercept. The % of hyperchromicity or hypochromicity (% H) for the CT DNA/[Ligand] was obtained from $(\epsilon_A - \epsilon_F) / \epsilon_F \cdot 100$.

2.3.4. *In silico* oral bioavailability assessment and ADME-toxicology studies

The oral bioavailability of the synthetic molecules (**3a-d**) can be predicted by considering their structural properties to screen based on the Rule of five or Lipinski rule-of-five (RO5) filter [33]. Rule of five employs the molecular properties necessary to filter candidate drug's pharmacokinetics (PK) and pharmacodynamics (PD) [34–36].

Oral bioavailability assessment was done using Osiris Data warrior V.4.4.3 [37] based on total molecular weight, ClogP, H-acceptors, H-donors, rotatable bonds as part of RO5 filters, along with TPSA (Topological polar surface area) and drug-likeness assessment [38]. Pharmacodynamic properties like mutagenicity, tumorigenicity, reproductive

effects, irritancy, Ames toxicity and hepatotoxicity were predicted using the admetSAR server. Bioactivity scores were predicted using the molinspiration server for GPCR ligand, ion channel modulator, kinase inhibitor, nuclear receptor inhibitor, protease inhibitor, enzyme inhibitor. Pharmacokinetic properties like blood-brain barrier penetration, human intestinal absorption, Caco-2 permeability and CYP450 2D6 substrate were predicted by submitting each molecule individually to the admetSAR server [39].

2.3.5. *In silico* molecular docking studies

The docking of the synthesized compounds to the binding pocket of glucosamine-6-phosphate synthase (GlcN-6-P) and P38 MAP kinase was carried out using the Autodock-Vina program [40]. The co-crystallized structure of GlcN-6-P (PDB ID: 2VF5) and P38 MAP kinase (PDB ID: 1OUK) were retrieved from protein databank, and their substrate binding sites were identified using pdbsum server [41, 42]. A grid box of dimensions 40 x 50 x 40 Å with X, Y and Z coordinates at 32.198, 16.709 and -3.151 for GlcN-6-P and 56 x 60 x 48 Å with X, Y and Z coordinates at 44.746, 34.234 and 32.603 for P38 MAPk were created respectively. For the obtained molecules, all the torsions were allowed to rotate during docking. The grid box was set around the residues forming the active pocket. The binding interactions were visualized using Biovia Discovery Studio Visualizer V.20.1 and Schrodinger-Maestro V.12.7. The *in silico* studies were performed on a local machine equipped with AMD Ryzen 5 six-core 3.4 GHz processor, 8 GB graphics and 16 GB RAM with Microsoft Windows 10 operating system.

2.3.6. Computational studies

Computational studies of synthesized compounds (**3a-d**) were conducted by using the Gaussian 09 software [43] with the help of the density functional theory at Becke-3-Lee-Yang-parr (DFT)/B3LYP level with 6-31G (d,p) basis set [44]. The energy minimization process has been conducted at the same level in the gas phase to obtain a stable structure. The 3D representation of the optimized structure was presented in a molecular visualization program Gauss view 5.0 and the output was processed using the Avogadro software [45].

3. Results and discussion

3.1. Chemistry

In this report, we developed a convenient and straightforward method for the synthesis of 5-(3-substituted-thiophene)-pyrimidine derivatives (**3a-d**) *via* Knoevenagel condensation of barbituric/thiobarbituric acid (**1**) with 3-substituted-thiophene-2-carboxaldehyde (**2**) in aqueous ethanol using $\text{H}_2\text{O}_2\text{:HCl}$ as catalyst (Scheme 1).

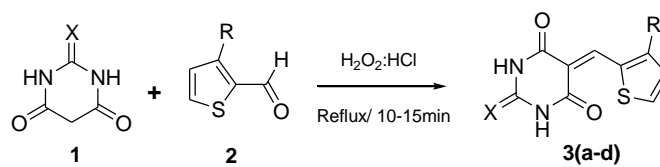
A possible mechanism for the formation of 5-(3-substituted-thiophene)-pyrimidine derivatives is shown in Scheme 2. Firstly, hypochlorous acid (HOCl) forms by the reaction of H_2O_2 with HCl, and it acts as a

powerful oxidizing agent. Then the reaction is initiated by the generation of carbanion **2** from active methylene compound **1**. The carbanion **2** attacks the carbonyl carbon of aldehyde **3** to form intermediate **4**, which undergo subsequent dehydration to desired Knoevenagel product **5**. HOCl increases the abstraction of acidic proton from active methylene compound and electrophilicity of carbonyl group of aldehydes due to hydrogen bonding.

Firstly, we studied the effect of catalyst on the reaction. In the previous reports, the same reaction was carried out in the presence of different catalysts such as CuO NPs, PVP-Ni NPs, Fe₃O₄ NPs, L-tyrosine, NH₂SO₃H, EAN, Bi(NO₃)₃·5H₂O, and also in the absence of catalyst (Table 1). We studied the influence of catalyst in the progress of reaction as well as on the increased product yield. The results were not very encouraging. Therefore, we concluded that the best result was obtained in the presence of green halogenating catalyst 6% H₂O₂:HCl, where a further increase in the quantity of catalyst doesn't significantly affect reaction kinetics.

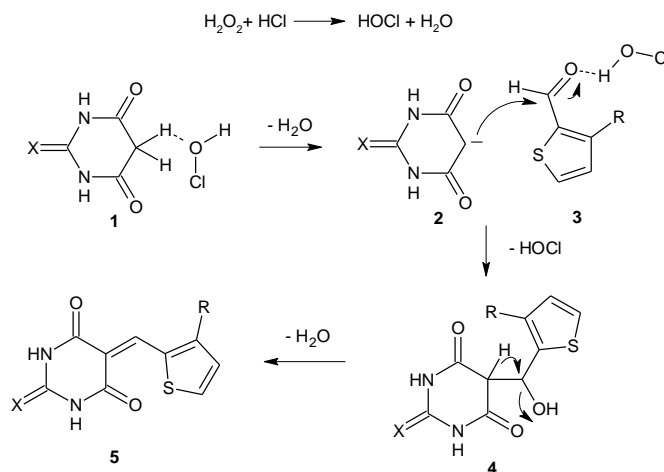
Consequently, to study the effect of temperature on synthesized compound **3a**, we carried out the reaction at room temperature, 50 °C and 80 °C (Table 2). As a result, an increase in the reaction temperature decreased the reaction time from 60 to 20 and 20 to 10 min, respectively. Still, the yield of the product was not affected by an increase in temperature.

The structures of the intended 5-(3-substituted-thiophene)-pyrimidine derivatives (**3a-d**) were confirmed by IR, ¹H NMR, ¹³C NMR and HRMS spectral data. IR spectrum of compound **3a** showed that the absorption band in the region 3373 cm⁻¹ is attributed to the amide stretching vibration, and the absorption band at 1654 cm⁻¹ corresponds to stretching vibration of the carbonyl group (C=O). Another stretching vibrational band at 1529 cm⁻¹ corresponds to C=C bond. The ¹H NMR spectrum of compound **3a** exhibited two singlet peaks at δ 11.21 and 11.17 ppm, which corresponds to two NH protons of pyrimidine nucleus (s, 2H, NH) and another singlet peak at δ 8.53 ppm due to CH proton (s, 1H, CH). A multiplet peak was observed in the range of δ 8.24–8.13 ppm, corresponds to two aromatic protons (m, 2H, Ar-H) and a triplet peak at 7.33–7.31 ppm due to one aromatic proton (t, *J* = 8 Hz, 1H, Ar-H).



X= O & S, R= H & CH₃

Scheme 1 Synthesis of 5-(3-substituted-thiophene)-pyrimidine derivatives (**3a-d**)



Scheme 2 Possible mechanism of synthesized compounds (**3a-d**)

In addition, the ¹³C NMR spectrum of compound **3a** exhibited peaks at δ 163.950 and 163.453 ppm, which correspond to carbonyl carbons.

The mass spectrum showed molecular ion peak [M+H]⁺ at *m/z* is 221. 9054 corresponds to the molecular weight of compound **3a** (Supporting information: S1 to S16). The physical and analytical data of synthesized compounds (**3a-d**) were appended in Table 3.

3.2. Pharmacological effect

3.2.1. Antibacterial activity

The synthesized 5-(3-substituted-thiophene)-pyrimidine derivatives (**3a-d**) were screened for their *in vitro* antibacterial activity at two different concentrations (20 and 40 µg/mL). All four compounds showed appreciable antibacterial activity with a varied zone of inhibition in the range of 3.3 to 3.8 and 7.1 to 7.8 mm against *E. coli* and 3.0 to 3.7 and 7.4 to 7.9 mm against *S. aureus*, respectively (Table 4).

Table 1 Effect of catalysts on synthesized compound **3a**

Entry	Catalyst	Solvent	Temperature, °C	Time, min	Yield, %
1	H ₂ O ₂ : HCl	EtOH:H ₂ O	Reflux	10	96
2	CuO NPs	-	RT	10	93 [46]
3	PVP-Ni NPs	Ethylene glycol	Reflux	10	87 [47]
4	Fe ₃ O ₄ NPs	EtOH	Reflux	30	70 [48]
5	L-tyrosine	H ₂ O	RT	16	93 [49]
6	NH ₂ SO ₃ H	-	Grinding	120	96 [50]
7	-	Ionic liquids	RT	10	96 [51]
8	Bi(NO ₃) ₃ ·5H ₂ O	EtOH	Reflux	20	95 [52]
9	-	EtOH	Reflux	120	89 [53]

Table 2 Effect of temperature on synthesized compounds **3a**

Entry	Temperature, °C	Time, min	Yield, %
1	RT	60	96
2	50	20	96
3	80	10	96

The results revealed that compounds **3b** (3.8 and 7.8 mm) and **3d** (3.7 and 7.9 mm) having electron-donating group (methyl) on C-3 of the thiophene ring exhibited the most inhibitory effect against bacterial strains *E. coli* and *S. aureus*, respectively, compared to the standard drug Ciprofloxacin.

3.2.2. Cytotoxicity

All the four synthesized compounds were investigated for their *in vitro* cytotoxicity against MCF-7 (Breast cancer) cell line (Fig. 2). The plot details compound concentration versus the survival fraction (Fig. 3). The percentages of cell survival of the tested compounds are listed in Table 5.

In vitro cytotoxicity results revealed that all four compounds displayed a superior selectivity against the MCF-7 cell line. Among the compounds tested, compound **3a** exhibited promising cytotoxicity with a minimum cell survival range of 23.68 to 44.16% at the concentration range of 200 to 6.25 µg/mL. Whereas **3b**, **3c** and **3d** displayed reliable selectivity at all the concentrations with cell sur-

vival ranges of 29.00 to 50.93%, 31.31 to 66.82% and 26.95 to 53.12%, respectively.

3.2.3. DNA binding study

DNA binding was assessed using electronic spectroscopy. The UV-absorption spectral studies were employed to examine the binding mode of compounds to CT DNA, which involves the changes in absorbance and wavelength [55]. The molecules are bound to DNA with two modes (covalent or non-covalent) of binding. The covalent binding led to bathochromism and hyperchromism due to breaking the DNA structure when a compound interacted with DNA covalently. While in non-covalent binding, there are "electrostatic", "groove", and "intercalative" types of interactions.

Table 4 Antibacterial activity results of synthesized compounds (**3a-d**)

Compd.	Zone of inhibition in mm			
	<i>Escherichia coli</i>		<i>Staphylococcus aureus</i>	
	Concentration in µg/mL			
	20	40	20	40
3a	3.5	7.8	3.0	7.5
3b	3.8	7.8	3.1	7.6
3c	3.3	7.2	3.5	7.4
3d	3.4	7.1	3.7	7.9
Ciprofloxacin	4.0	8.0	4.2	8.4

Table 3 Physical and analytical data of synthesized compounds (**3a-d**)

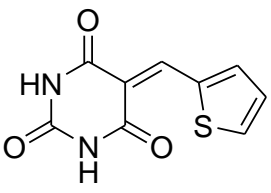
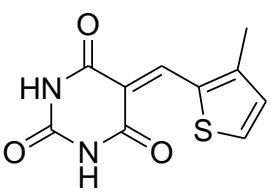
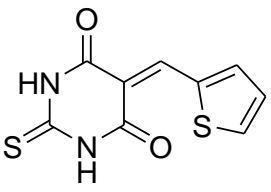
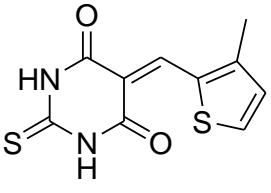
Entry	Comp.	X	R	Product	Yield (%)	MP (°C)	
						Observed	Reported
1	3a	O	H		98	278-280	271 [54]
2	3b	O	CH ₃		95	302-306	-
3	3c	S	H		94	320-322	-
4	3d	S	CH ₃		96	310-312	-



Fig. 2 Images of anticancer study of the synthesized compounds (3a-d)

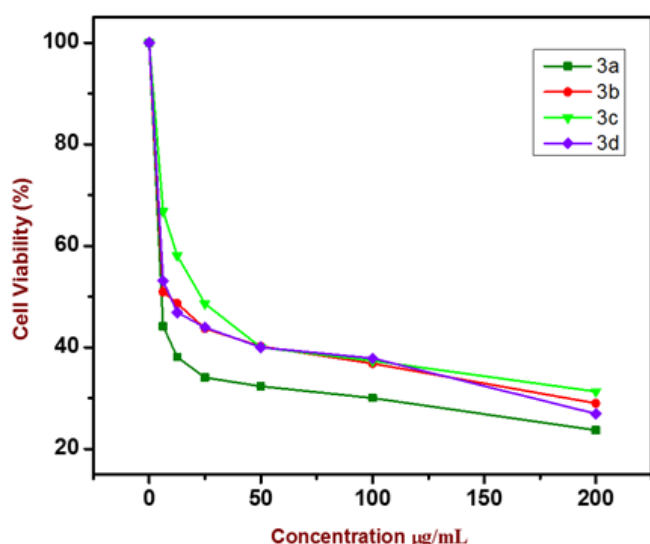


Fig. 3 A graph of % of surviving cells of compounds (3a-d) at different concentration against MCF-7 cell line

Table 5 Percentage of cell viability against MCF-7 cell line of the synthesized compounds (3a-d)

Concentration in µg/mL	Mean cell Viability of MCF-7			
	3a	3b	3c	3d
6.25	44.16±0.76	50.93±0.42	66.82±0.41	53.12±0.34
12.5	38.11±0.82	48.68±0.31	58.1±0.13	46.88±0.52
25	34.09±1.2	43.72±0.52	48.6±0.23	43.93±0.42
50	32.37±0.82	40.23±0.61	40.03±0.82	40.03±0.62
100	30.06±0.62	36.80±0.20	37.38±0.61	37.85±0.34
200	23.68±0.41	29.00±0.16	31.31±0.42	26.95±0.52

Values are Mean ±SE, N=3, *P<0.01 vs. Control

Decreased absorption (hypochromic shifts) and red-shift (bathochromic shift) revealed the intercalative binding of compounds with DNA. Lower hypochromic/hyperchromic effect with no or negligible bathochromic shift led to the electrostatic binding. Minor or no effect and, rarely, some hyperchromism show the groove binding [56–58].

The DNA binding efficiency of synthesized compounds (3a-d) was monitored by comparing their absorption spectra with and without CT DNA. The absorption spectra were carried out at a fixed concentration of synthesized compounds and varying with DNA concentrations (25–350 µL of $0.5025 \cdot 10^{-7}$ to $6.0670 \cdot 10^{-7}$ mol L⁻¹) under the physiological condition of pH 7.01. The absorption spectra of all the synthesized compounds (3a-d) exhibited absorption bands at 235 to 240 nm due to π - π^* transitions (Fig. 4). The K_b values of compounds (3a-d) are found to be $1.1216 \cdot 10^7$, $1.4072 \cdot 10^7$, $1.0634 \cdot 10^7$ and $3.4872 \cdot 10^7$ respectively are shown in Table 6. These K_b values confirm that all the synthesized compounds interacted strongly with CT DNA. Among the four compounds, compound 3d showed a prominent binding ability with CT DNA compared to other compounds. The absorption bands of the compounds were affected due to the gradual increase of CT DNA concentration resulting hyperchromism/hypochromism. No/or negligible blue/red shift indicates strong interaction of the compounds with CT DNA mainly through electrostatic or groove binding [59]. The kinetics and thermodynamics of compounds-DNA interaction in terms of binding constant (K_b) and Gibbs free energy change (ΔG) were evaluated using the classical Van't Hoff's equation, $\Delta G = -2.303RT \log K_b$. The negative ΔG values confirmed spontaneous binding of compounds with CT DNA through the formation of stable complexes.

3.2.4. *In silico* ADME-toxicology studies

The bioavailability and drug-likeness were estimated for all the synthesized compounds (3a-d) based on the molecular properties. The results indicated that all the four compounds under study could pass through Lipinski's filter without any violation, demonstrating a positive drug-likeness score indicating their suitability as drug-leads. *In silico* pharmacokinetic studies showed that all the molecules under investigation could penetrate the blood-brain barrier and are readily absorbed by the human intestine while they are impermeable to Caco-2, and non-substrate Cytochromes P450 (CYP450) group of enzymes (Table 7).

Table 6 DNA binding results of synthesized compounds (3a-d)

Compd.	λ_{max} , nm		$\Delta\lambda_{max}$, nm	% H	K_b , M ⁻¹	ΔG , kJ/mol
	Free	Bound				
3a	240	239	1	$6.1879 \cdot 10^{-4}$	$1.1216 \cdot 10^7$	-40.205
3b	236	236	0	$6.0157 \cdot 10^{-4}$	$1.4072 \cdot 10^7$	-40.767
3c	239	239	0	$1.1560 \cdot 10^{-3}$	$1.0634 \cdot 10^7$	-40.073
3d	236	236	0	$1.2388 \cdot 10^{-3}$	$3.4872 \cdot 10^7$	-43.015

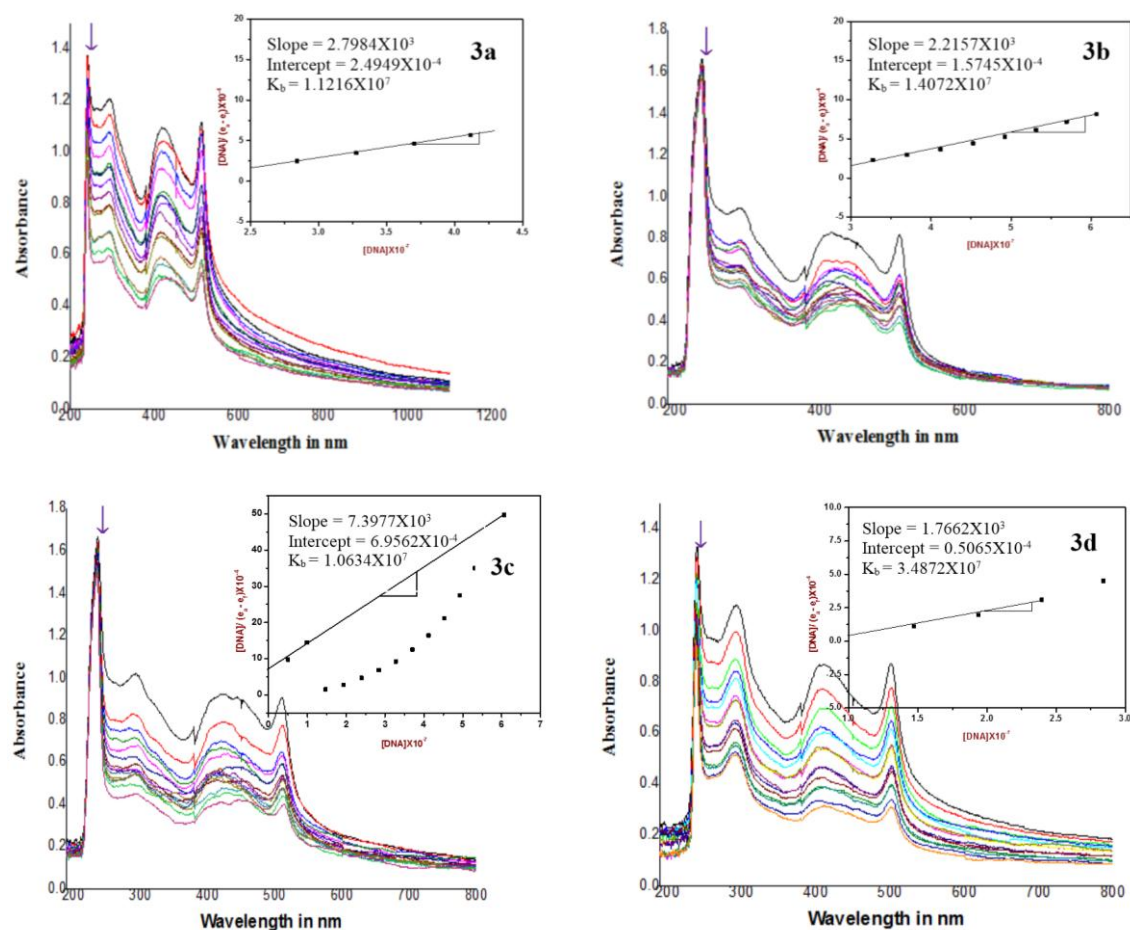


Fig. 4 The electronic absorption spectra of compounds (**3a-d**) in the absence and presence of increasing amounts of CT DNA. Arrow (↓) shows the change in the absorbance with increase the DNA concentration. Inset: plot of $[DNA]/(\epsilon_A - \epsilon_F)$ Vs $[DNA]$

Table 7 Bioavailability, drug likeness and *in silico* pharmacokinetic assessment of synthesized compounds (**3a-d**)

Comp.	Bioavailability and Drug likeness					<i>In silico</i> Pharmacokinetics					
	Total Molecular weight	cLogP	H-Acceptors	H-Donors	Rotatable Bonds	Polar Surface Area	Drug likeness	Human intestinal absorption	Caco-2 permeability	Blood brain barrier	CYP450 2D6 substrate
3a	222.224	0.2739	5	2	1	103.51	5.2698	+0.982	-0.779	+0.982	-0.873
3b	236.251	0.6178	5	2	1	103.51	4.9763	+0.728	-0.753	+0.980	-0.889
3c	238.291	0.6344	4	2	1	118.53	4.2229	+0.979	-0.698	+0.977	-0.871
3d	252.318	0.9783	4	2	1	118.53	3.9143	+0.987	-0.673	+0.976	-0.886

In silico pharmacodynamics studies revealed that all the four molecules are non-mutagenic, non-tumorigenic, non-irritant, AMES non-toxic with high reproductive effects with possible hepatotoxicity. The bioactivity assessment indicated that the molecules do not belong to the GPCR group of ligands, do not modulate ion channels, non-kinase inhibitors, non-nuclear receptor ligands, non-protease and non-enzyme inhibitors (Table 8).

3.2.5. Structure-activity relationship (SAR) studies

The evaluation of the antibacterial activity of the newly synthesized compounds (**3a-d**) revealed that the presence

of electron-donating methyl group has a significant effect on enhancing their potency. The compounds **3b** and **3d** have a methyl group at C-3 of the thiophene ring. This could have improved their cell permeability, which improved their activity profile compared to **3a** and **3c**. The combination of heterocyclic rings like pyrimidine and thiophene is presumed to be the main reason for the profound cytotoxicity of the newly synthesized compounds (**3a-d**). Furthermore, the presence of the urea group in the pyrimidine ring could have significantly contributed to the superior cytotoxicity of **3a** and **3b** compared to other synthesized molecules.

3.2.6. In silico molecular docking studies

The results revealed that compound **3b** bound with GlcN-6-P and P38 MAPk with a minimum binding energy of -7.9 and -6.4 kcal/mol, respectively. **3a**, **3d** and **3c** interacted with a binding energy of -7.6 and -6.4, -7.4 and -6.2 and -7.4 and -6.0 with GlcN-6-P and P38 MAPk targets, respectively. The interaction of all the molecules with GlcN-6-P and P38 MAPk were compared with antibacterial agent Ciprofloxacin (-7.7 kcal/mol) and anticancer agent 5-fluorouracil (-4.7 kcal/mol) (Table 9, Fig.5). The computational methods in drug discovery have gained enormous importance in modern drug research. They play a critical role in reducing the virtual chemical space in synthesizing, modifying, and screening chemical drugs against a specific disease target. Their effectiveness can be validated using microbial pathogens due to their simpler and clearer cellular understandings. Similarly, cell death modalities can also be studied using *in vitro* cell culture studies, particularly focusing on necrosis, apoptosis, necroptosis, autophagic cell death, etc. [42]. In the present study, *in silico* molecular docking studies were performed to predict the most effective binding among the synthesized molecules to appropriate targets [60, 61]. The studied molecules showed remarkable binding interactions with the selected target proteins, supporting their remarkable antimicrobial and anticancer effects.

3.2.7. DFT studies

Frontier molecular orbitals (FMOs) containing the highest occupied molecular orbital (HOMO) and lowest unoccupied molecular orbital (LUMO), as well as the energy gap ($\Delta E = E_{\text{HOMO}} - E_{\text{LUMO}}$) were considered to be very effective parameters in chemical quantum chemistry [62]. FMOs also delivered important information about chemical reactivity, biological activity and kinetic stability of the molecules [63]. The optimized HOMO and LUMO structures of synthesized compounds (**3a-d**) are shown in Fig. 6 and 7. The HOMO and LUMO of compounds were helpful in determining of various global reactivity parameters such as ionization energy ($I = -E_{\text{HOMO}}$), electron affinity ($A = -E_{\text{LUMO}}$), chemical hardness ($\eta = 1/2 (I - A)$), chemical softness ($\sigma = 1/\eta$), electronegativity ($\chi = 1/2 (I + A)$), chemical potential ($\mu = -\chi$), and electrophilicity index ($\omega = \mu^2/2\eta$) helps to study about donor-

acceptor interaction and intramolecular charge transfer (ICT) ability of synthesized compounds [64].

The calculated HOMO-LUMO energies and global reactivity parameters of the synthesized compounds (**3a-d**) are displayed in Table 10. A smaller HOMO-LUMO energy gap (ΔE) indicates a soft molecule, while a larger gap indicates a hard molecule. Lower energy gap, less ionization potential, electron affinity, chemical hardness, electronegativity, electrophilicity index values and more softness values indicate that a molecule is more chemically and biologically active with low kinetic stability [65].

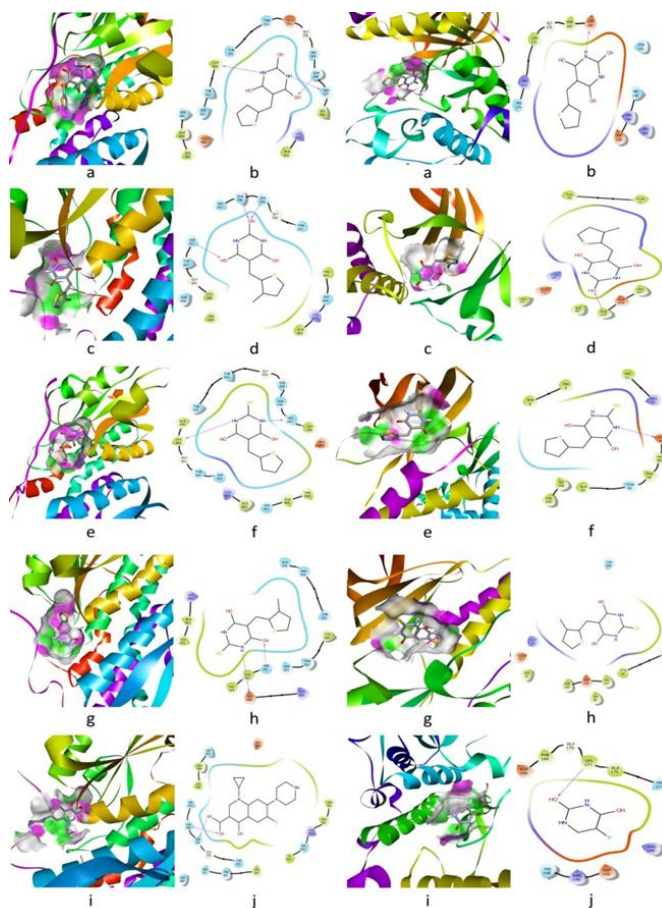


Fig. 5 Binding interaction of compounds **3a** (a and b), **3b** (c and d), **3c** (e and f), and **3d** (g and h) with GlcN-6-P along with standard drug ciprofloxacin (i and j) (a) and Binding interaction of compounds **3a** (a and b), **3b** (c and d), **3c** (e and f), and **3d** (g and h) with P38 MAPk along with standard drug 5-fluorouracil (i and j) (b)

Table 8 *In silico* pharmacodynamics and bioactivity assessment of synthesized compounds (**3a-d**)

Comp.	<i>In silico</i> Pharmacodynamics							Bioactivity score					
	Mutagenic	Tumorigenic	Reproductive Effective	Irritant	Aerobic biodegradability	Ames toxicity	Hepatotoxicity	GPCR ligand	Ion channel modulator	Kinase inhibitor	Nuclear receptor ligand	Protease inhibitor	Enzyme inhibitor
3a	NONE	NONE	HIGH	NONE	-0.590	-0.706	+0.925	-1.12	-1.58	-0.86	-1.26	-1.30	-0.69
3b	NONE	NONE	HIGH	NONE	-0.562	-0.694	+0.950	-1.07	-1.44	-0.90	-0.91	-1.32	-0.73
3c	HIGH	NONE	HIGH	NONE	-0.859	-0.731	+0.900	-1.43	-1.77	-1.41	-1.73	-1.32	-1.00
3d	HIGH	NONE	HIGH	NONE	-0.843	-0.711	+0.850	-1.35	-1.62	-1.42	-1.35	-1.34	-1.03

DFT studies data reveals that the energy gaps (ΔE) of compounds **3a**, **3b**, **3c** and **3d** are 0.16038 eV, 0.15988 eV, 0.12799 eV and 0.12636 eV, respectively. **3a**, **3b** and **3c**, **3d** molecules show nearly similar energy gap due to the similar structure. Among them **3d** molecule shows less energy gap (0.12636 eV) and more softness value (15.8277 eV); hence, it is chemically more reactive compared to the other molecules. **3a** molecule has more electronegative value (0.19923 eV); hence, it has more tendency to attract a bonding electron pairs compared to the other molecules.

Table 9 Binding energies of synthesized compounds (**3a-d**) with GlcN-6-P and P38 MAPK targets

Antibacterial activity		Anticancer activity	
Compd.	Binding energy in kcal/mol	Compd.	Binding energy in kcal/mol
Ciprofloxacin	-7.7	5-Fluorouracil	-4.7
3a	-7.6	3a	-6.4
3b	-7.9	3b	-6.4
3c	-7.4	3c	-6.0
3d	-7.4	3d	-6.2

Table 10 Chemical parameters of synthesized compounds (**3a-d**)

Entry	E_{HOMO} (eV)	E_{LUMO} , eV	ΔE $E_{\text{HOMO}} - E_{\text{LUMO}}$, eV	I , eV	A , eV	η , eV	σ , eV	χ , eV	μ , eV	ω , eV	D , Debye
3a	-0.27942	-0.11904	0.16038	0.27942	0.11904	0.08019	12.4703	0.19923	-0.19923	0.24749	4.6744
3b	-0.27411	-0.11423	0.15988	0.27411	0.11423	0.07994	12.5093	0.19417	-0.19417	0.23581	5.2238
3c	-0.25095	-0.12296	0.12799	0.25095	0.12296	0.06399	15.6274	0.18695	-0.18695	0.27310	5.4300
3d	-0.24793	-0.12157	0.12636	0.24793	0.12157	0.06318	15.8277	0.18475	-0.18475	0.27012	5.9267

Conclusions

We described a mild, easy and green protocol for synthesizing 5-(3-substituted-thiophene)-pyrimidine derivatives (**3a-d**) using $\text{H}_2\text{O}_2:\text{HCl}$ as a catalyst under reflux condition. This synthetic approach has a short reaction time, excellent yield, and clean reactions make this procedure a magnificent alternative to the existing methods. Furthermore, this method is environmentally greener and safer. The activity results revealed that the compounds **3b** and **3d** exhibited more potent antibacterial activity against *E. coli* and *S. aureus* than the standard drug Ciprofloxacin. *In vitro* cytotoxicity results disclosed the outstanding selectivity on MCF-7 cell line, mainly compound **3a** exhibiting the most effective cytotoxicity with a minimum cell survival range of 23.68 to 44.16%. DNA binding results indicated that all the synthesized compounds interacted strongly with CT DNA, and compound-DNA complexes were stabilized by electrostatic or groove binding. *In silico* ADME-toxicology results showed that all the four compounds are non-toxic and suitable for oral bioavailability and drug-likeness, indicating their suitability as drug-leads.

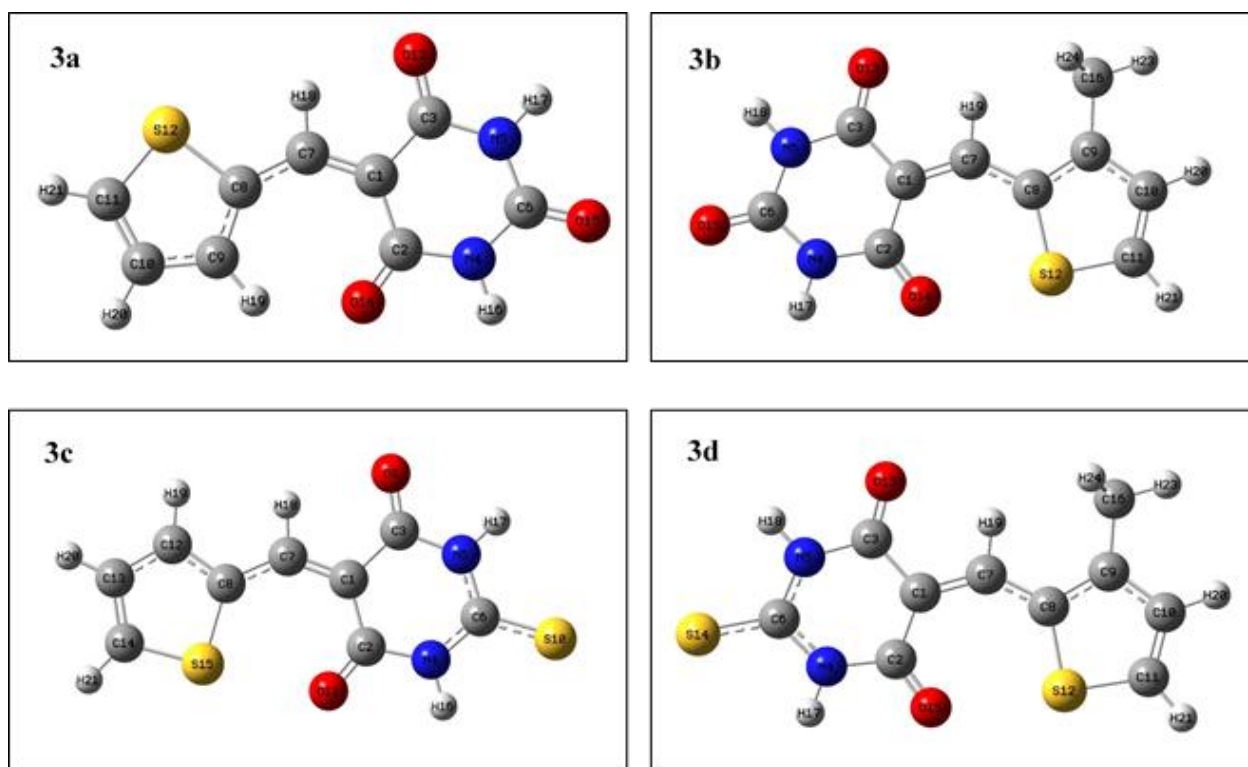


Fig. 6 Optimized structures of synthesized compounds (**3a-d**)

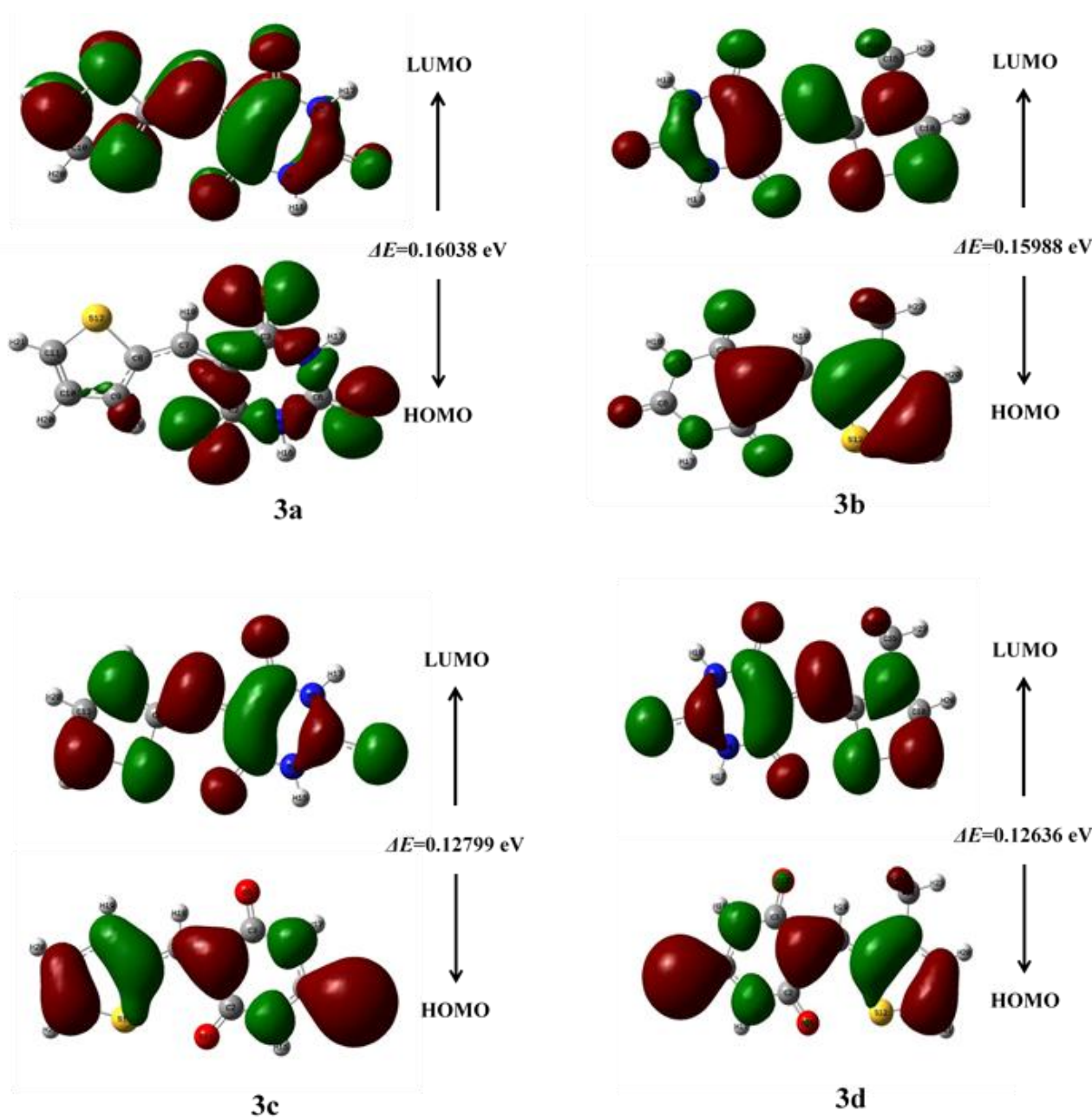


Fig. 7 DFT study of synthesized compounds (**3a-d**)

In silico molecular docking results showed compound **3b** bound with GlcN-6-P and P38 MAPk with a least binding energy of -7.9 and -6.4 kcal/mol, respectively. DFT study result revealed that the compound **3d** was chemically and biologically more reactive with low kinetic stability due to less energy gap. In future, the obtained compounds can be used as antibiotics, anticancer agents, dyes and pigments in compounds as food industries.

Acknowledgements

The authors are thankful to the Chairman, Department of Chemistry, Kuvempu University, Shankaraghatta, for providing the laboratory facilities and SAIF, Mysore University, for providing the spectral data.

Supporting information

Spectroscopic spectra's (IR, ^1H NMR, ^{13}C NMR and HRMS) of the synthesized compounds are provided in the supporting information file.

Conflict of Interest

The authors declare that there is no conflict of interests regarding the publication of this work.

References

1. Singh PK, Silakari O. The current status of O-heterocycles: A synthetic and medicinal overview. *Med Chem.* 2018;13:1071-1087. doi:[10.1002/cmdc.201800119](https://doi.org/10.1002/cmdc.201800119)
2. Pathania S, Narang RK, Rawal RK. Role of sulphur-heterocycles in medicinal chemistry: An update. *Eur J Med Chem.* 2019;180:486-508. doi:[10.1016/j.ejmech.2019.07.043](https://doi.org/10.1016/j.ejmech.2019.07.043)

3. Venkatesh T, Bodke YD, Manjunatha B, Kumar SR. Synthesis, antitubercular activity and molecular docking study of substituted [1,3]dioxino[4,5-d] pyrimidine derivatives via facile CAN catalyzed Biginelli reaction. *Nucleosides, Nucleotides and Nucleic Acids*. 2021;1-13. doi:[10.1080/15257770.2021.1972310](https://doi.org/10.1080/15257770.2021.1972310)
4. Sravanthi B, Kaviarasan L, Praveen TK, Sai Kiran PSS, Pavankumar C, Gowramma B. Synthesis and pharmacological evaluation of 1,3,4-thiadiazole bearing pyrimidine derivatives as STAT3 inhibitor for treatment of breast cancer. *J Iran Chem Soc*. 2020;17:2359-2370. doi:[10.1007/s13738-020-01932-z](https://doi.org/10.1007/s13738-020-01932-z)
5. Kang D, Feng D, Ginex T, Zou J, Wei F, Zhao T, Huang B, Sun Y, Desta S, Clercq ED, Pannecouque C, Zhan P, Liu X. Exploring the hydrophobic channel of NNIBP leads to the discovery of novel piperidinesubstituted thiophene[3,2-d]pyrimidine derivatives as potent HIV-1 NNRTIs. *Acta Pharm Sin B*. 2020;10:878-894. doi:[10.1016/j.apsb.2019.08.013](https://doi.org/10.1016/j.apsb.2019.08.013)
6. Prasad P, Anirudhdha GK and Patel MP. Microwave assisted one-pot synthetic route to imidazo[1,2-a]pyrimidine derivatives of imidazo/triazole clubbed pyrazole and their pharmacological screening. *New J Chem*. 2018;42:12666-12676. doi:[10.1039/C8NJ00670A](https://doi.org/10.1039/C8NJ00670A)
7. Zia UHK, Arif UK, Pingyu W, Yongmei C, Dandan K, Shafullah K, Kamran T. In vitro pharmacological screening of three newly synthesised pyrimidine derivatives. *Nat Prod Res*. 2015;29:933-938. doi:[10.1080/14786419.2014.964707](https://doi.org/10.1080/14786419.2014.964707)
8. Ghada SM. New Potential Antitumor Pyrimidine Derivatives: Synthesis and Cytotoxicity Evaluation. *Polycycl Aromat Compd*. 2021:1-17. doi:[10.1080/10406638.2021.1936086](https://doi.org/10.1080/10406638.2021.1936086)
9. Zhen X, Cilong C, Lingjia Z, Zhihui Z, Qian Z, Feiyi Y, Zunhua Y, Pengwu Z, Shan X, Wufu Z. Discovery of thiapyran-pyrimidine derivatives as potential EGFR inhibitors. *Bioorg Med Chem*. 2020;28:1-13. doi:[10.1016/j.bmc.2020.115669](https://doi.org/10.1016/j.bmc.2020.115669)
10. Zhen X, Zhihui Z, Cilong C, Qian Z, Lingjia Z, Zunhua Y, Xin Li, Liying Yu, Pengwu Z, Shan Xu, Wufu Z. Design, synthesis and antitumor activity of novel thiophene-pyrimidine derivatives as EGFR inhibitors overcoming T790M and L858R/T790M mutations. *Eur J Med Chem*. 2020;203:1-43. doi:[10.1016/j.ejmech.2020.112511](https://doi.org/10.1016/j.ejmech.2020.112511)
11. Elshaymaa IE. Thieno[2,3-d]pyrimidine derivatives: Synthetic approaches and their FLT3 kinase inhibition. *J Heterocyclic Chem*. 2020;57:2067-2078. doi:[10.1002/jhet.3934](https://doi.org/10.1002/jhet.3934)
12. Khalil NA, Ahmed EM, Zaher AF, El-Zoghbi MS, Sobh EA. Synthesis of certain benzothieno[3,2-d]pyrimidine derivatives as a selective SIRT2 inhibitors. *Eur J Med Chem*. 2020;187:1-56. doi:[10.1016/j.ejmech.2019.111926](https://doi.org/10.1016/j.ejmech.2019.111926)
13. Shipilovskikh SA, Rubtsov AE. One-Pot Synthesis of Thieno[3,2-e]pyrrolo[1,2-a]pyrimidine Derivative Scaffold: A Valuable Source of PARP-1 Inhibitors. *J Org Chem*. 2019;84:15788-15796. doi:[10.1021/acs.joc.9b00711](https://doi.org/10.1021/acs.joc.9b00711)
14. Lei S, Chengjuan C, Xueting H, Hao H, Manman W, Jianqiu Z, Yile Y, Jianming L, Tiantai Z, Dayong Z. Design, synthesis, and pharmacological evaluation of 4- or 6-phenylpyrimidine derivatives as novel and selective Janus kinase 3 inhibitors. *Eur J Med Chem*. 2020;191:1-18. doi:[10.1016/j.ejmech.2020.112148](https://doi.org/10.1016/j.ejmech.2020.112148)
15. Giuseppe R, Loredana S, Valeria P, Marialuisa C, Sebastiano I, Emanuele A, Mario S, Alfredo C, Antonio R, Giuseppe F, Maria NM. [1]Benzothieno[3,2-d]pyrimidine derivatives as ligands for the serotonergic 5-HT7 receptor. *Eur J Med Chem*. 2019;183:1-16. doi:[10.1016/j.ejmech.2019.111690](https://doi.org/10.1016/j.ejmech.2019.111690)
16. Ali I, Wani WA, Saleem K, Hsieh MF. Anticancer metallodrugs of glutamic acid sulphonamides: in silico, DNA binding, hemolysis and anticancer studies. *RSC Adv*. 2014;4:29629-29641. doi:[10.1039/C4RA02570A](https://doi.org/10.1039/C4RA02570A)
17. Aarti A, Archana K, Dr. Amarjit KA, Dr. Nithish C, Yudhvirs. Recent advances made on anticancer drugs the therapeutic potential of the aromatic heterocyclic compounds. *Int J Pharm Sci Rev Res*. 2019;58:104-113.
18. Jawaid A, Ahsan AK, Zulphikar Ali, Rafi H, Shahar YM. Structure-activity relationship (SAR) study and design strategies of nitrogen-containing heterocyclic moieties for their anticancer activities. *Eur J Med Chem*. 2017;125:143-189. doi:[10.1016/j.ejmech.2016.09.023](https://doi.org/10.1016/j.ejmech.2016.09.023)
19. Prabodh CS, Kushal KB, Archana S, Diksha S, Aakash D. Thiazole-containing compounds as therapeutic targets for cancer therapy. *Eur J Med Chem*. 2020;188:1-47. doi:[10.1016/j.ejmech.2019.112016](https://doi.org/10.1016/j.ejmech.2019.112016)
20. Garima M, Sumitra N, Pramod KS. Cancer: An overview. *J Cancer Res*. 2015;8:1-9. doi:[10.5829/idosi.ajcr.2015.8.1.9336](https://doi.org/10.5829/idosi.ajcr.2015.8.1.9336)
21. Nathan MR and Schmid P. A review of fulvestrant in breast cancer. *Oncol Ther*. 2017;5:17-29. doi:[10.1007/s40487-017-0046-2](https://doi.org/10.1007/s40487-017-0046-2)
22. Akhtar J, Khan AA, Ali Z, Haider R, Yar MS. Structure-activity relationship (SAR) study and design strategies of nitrogen containing heterocyclic moieties for their anticancer activities. *Eur J Med Chem*. 2016;125:143-189. doi:[10.1016/j.ejmech.2016.09.023](https://doi.org/10.1016/j.ejmech.2016.09.023)
23. Koohshari M, Dabiri M, Salehi P. Catalyst-free domino reaction in water/ethanol: an efficient, regio- and chemoselective one-pot multi-component synthesis of pyranopyrazole derivatives. *RSC Adv*. 2014;4:10669-10671. doi:[10.1039/C3RA47639A](https://doi.org/10.1039/C3RA47639A)
24. Daniel RB, De Visser SP, Shaik S, Neumann R. Electrophilic aromatic chlorination and haloperoxidation of chloride catalyzed by polyfluorinated alcohols: a new manifestation of template catalysis. *J Am Chem Soc*. 2003;125:12116-12117. doi:[10.1021/ja0364524](https://doi.org/10.1021/ja0364524)
25. Venkatesh T, Bodke YD, Nagaraj K, Kumar SR. One-pot synthesis of novel substituted phenyl-1,5-dihydro-2H-benzo[4,5]thiazolo[3,2-a]pyrimido[4,5-d]pyrimidine derivatives as potent antimicrobial agents. *Med Chem*. 2018;8:1-7. doi:[10.4172/2161-0444.1000488](https://doi.org/10.4172/2161-0444.1000488)
26. Venkatesh T, Bodke YD, Kenchappa R, Telkar S. Synthesis, antimicrobial and antioxidant activity of chalcone derivatives containing thiobarbitone nucleus. *Med Chem*. 2016;6:440-448. doi:[10.4172/2161-0444.1000383](https://doi.org/10.4172/2161-0444.1000383)
27. Sukanya SH, Venkatesh T, Kumar SR, Bodke YD. Facile TiO₂ NPs catalysed synthesis of substituted-4-Hydroxy/methoxy benzylidene derivatives as potent antioxidant and antitubercular agents. *Chem Data Collect*. 2021;33:1-16. doi:[10.1016/j.cdc.2021.100713](https://doi.org/10.1016/j.cdc.2021.100713)
28. Venkatesh T, Bodke YD, Joy NM, Vinoda BM, Shiralgi Y, Dhananjaya BL. Synthesis of some novel 5,7-disubstituted-2-phenyl-5H-[1,3,4]thiadiazolo[3,2-a]pyrimidine derivatives and evaluation of their biological activity. *Lett Org Chem*. 2016;13:661-671. doi:[10.2174/1570178613666161017123123](https://doi.org/10.2174/1570178613666161017123123)
29. Sukanya SH, Venkatesh T, Aditya Rao SJ, Joy MN. Efficient L-Proline catalyzed synthesis of some new (4-substituted-phenyl)-1,5-dihydro-2H-pyrimido[4,5-d][1,3]thiazolo[3,2a]-pyrimidine-2,4(3H)-diones bearing thiazolopyrimidine derivatives and evaluation of their pharmacological activities. *J Mol Struct*. 2021;1247:1-13. doi:[10.1016/j.molstruc.2021.131324](https://doi.org/10.1016/j.molstruc.2021.131324)
30. Shivakumara N, Murali Krishna P. Synthesis, Spectral Characterization, and Evaluation of their DNA interactions. *Curr Chem Lett*. 2019;8:157-168. doi:[10.5267/j.ccl.2019.004.004](https://doi.org/10.5267/j.ccl.2019.004.004)
31. Ali I, Mukhtar SD, Hsieh MF, Allothman ZA, Alwarthan A. Facile synthesis of indole heterocyclic compounds based micellarnano anticancer drugs. *RSC Adv*. 2018;8:37905-37914. doi:[10.1039/c8ra07060a](https://doi.org/10.1039/c8ra07060a)
32. Wolfe A, Shimer GH, Meehan T. Polycyclic aromatic hydrocarbons physically intercalate into duplex regions of denatured DNA. *Biochemistry*. 1987;26:6392-6396.
33. Lipinski CA, Lombardo F, Dominy BW, Feeney PJ. Experimental and computational approaches to estimate solubility and permeability in drug discovery and development settings. *Adv Drug Deliv Rev*. 1997;23:3-25. doi:[10.1016/S0169-409X\(96\)00423-1](https://doi.org/10.1016/S0169-409X(96)00423-1)
34. Aditya R, Venugopal T, Jayanna N, Pamesha M, Ramesh C. Bioactive isolates of Morus species as antibacterial agents and their insilico profiling. *Lett. Drug Des Discov*. 2020;17:1-9. doi:[10.2174/1570180817999201104120815](https://doi.org/10.2174/1570180817999201104120815)

35. Jarrahpour A, Motamedifar M, Zarei M, Youssoufi MH, Mimouni M, Chohan ZH. Petra, Osiris, and Molinspiration together as a guide in drug design: Predictions and correlation structure/antibacterial activity relationships of new n-sulfonyl monocyclic β -Lactams. Phosphorus Sulfur Silicon Relat Elem. 2010;185:491-497. doi:[10.1080/10426500902953953](https://doi.org/10.1080/10426500902953953)
36. Raghavendra S, Aditya Rao SJ, Kumar V, Ramesh CK. Multiple ligand simultaneous docking (MLSD): A novel approach to study the effect of inhibitors on substrate binding to PPO. Comput Biol Chem. 2015;59:81-86. doi:[10.1016/j.compbiolchem.2015.09.008](https://doi.org/10.1016/j.compbiolchem.2015.09.008)
37. Sander T, Freyss J, Von Korff M, Rufener C. DataWarrior: An open-source program for chemistry aware data visualization and analysis. J Chem Inf Model 2015;55:460-473. doi:[10.1021/ci500588j](https://doi.org/10.1021/ci500588j)
38. Venkatesh T, Bodke YD, Aditya Rao SJ. Facile CAN catalyzed one pot synthesis of novel indol-5,8-pyrimido[4,5-d]pyrimidine derivatives and their pharmacological study. Chem Data Collect. 2020;25:1-13. doi:[10.1016/j.cdc.2019.100335](https://doi.org/10.1016/j.cdc.2019.100335)
39. Cheng F, Li W, Zhou Y, Shen J, Wu Z, Liu G. AdmetSAR. A comprehensive source and free tool for assessment of chemical ADMET properties. J Chem Inf Model. 2012;52:3099-3105. doi:[10.1021/ci300367a](https://doi.org/10.1021/ci300367a)
40. Trott O, Olson JA. AutoDockVina: Improving the speed and accuracy of docking with a new scoring function, efficient optimization and multithreading. J Comput Chem. 2010;31:455-461. doi:[10.1002/jcc.21334](https://doi.org/10.1002/jcc.21334)
41. Aditya Rao SJ, Ramesh CK, Raghavendra S, Paramesha M. Dehydroabietylamine, A diterpene from *carthamus tinctorius* L. showing antibacterial and anthelmintic effects with computational evidence. Curr Comput Aided Drug Des. 2020;16:231-237. doi:[10.2174/1573409915666190301142811](https://doi.org/10.2174/1573409915666190301142811)
42. Aditya Rao SJ, Shivayogi SM, Satyanarayana JK, Kumaran RC. Characterization of isolated compounds from *Morus* spp. and their biological activity as anticancer molecules. Bioimpacts 2021;11:1-11. doi:[10.34172/bi.2021.09](https://doi.org/10.34172/bi.2021.09)
43. Frisch MJE, Trucks GW, Schlegel HB, Scuseria GE, Robb MA, Cheeseman JR, Nakatsuji H. Gaussian 09, Revision d. 01, Gaussian, Inc. Wallingford CT 2009;201.
44. Becke AD. A new mixing of Hartree-Fock and local density-functional theories. J Chem Phys. 1993;98:1372-1377.
45. Hanwell MD, Curtis DE, Lonie DC, Vandermeersch T, Zurek E, Hutchison GR. Avogadro an advanced semantic chemical editor, visualization, and analysis platform. Aust J Chem. 2012;4:1-33. doi:[10.1186/1758-2946-4-17](https://doi.org/10.1186/1758-2946-4-17)
46. Dighore NR, Anandgaonker PL, Gaikwad ST, Rajbhoj AS. Solvent free green synthesis of 5-arylidene barbituric acid derivatives catalyzed by copper oxide nanoparticles. Res J Chem Sci. 2014;4:93-98.
47. Khurana JM, Kanika V. Nickel nanoparticles catalyzed knoevenagel condensation of aromatic aldehydes with barbituric acids and 2-thiobarbituric acids. Catal Lett. 2010;138:104-110. doi:[10.1007/s10562-010-0376-2](https://doi.org/10.1007/s10562-010-0376-2)
48. Fattahi M, Davoodnia A, Pordel M. Efficient one-pot synthesis of some new pyrimido[5,4:5,6]pyrido[2,3-d]pyrimidines catalyzed by magnetically recyclable Fe₃O₄ nanoparticles. Russ J Gen Chem. 2017;87:863-867. doi:[10.1134/S1070363217040326](https://doi.org/10.1134/S1070363217040326)
49. Thirupathi G, Venkatanarayana M, Dubey PK, BharathiKumari Y. Facile and green syntheses of 5-arylidene-pyrimidine-2,4,6-triones and 5-arylidene-2-thioxo-dihydro-pyrimidine-4,6-diones using L-tyrosine as an efficient and eco-friendly catalyst in aqueous medium. Chem Sci Trans. 2013;2:441-446. doi:[10.7598/cst2013.385](https://doi.org/10.7598/cst2013.385)
50. Tai Li J, Guang Dai H, Liu D, Shuang Li T. Efficient method for synthesis of the derivatives of 5-arylidene barbituric acid catalyzed by aminosulfonic acid with grinding. Synth Commun. 2006;36:789-794. doi:[10.1080/00397910500451324](https://doi.org/10.1080/00397910500451324)
51. Hu Y, Chen ZC, Le ZG, Zheng QG. Organic reactions in ionic liquids: ionic liquid promoted knoevenagel condensation of aromatic aldehydes with (2-thio) barbituric acid. Synth Commun. 2004;34:4521-4529. doi:[10.1081/SCC-200043210](https://doi.org/10.1081/SCC-200043210)
52. Shabeer M, Barbosa LCA, Karak M, Coelho ACS. Thiobarbiturates as potential antifungal agents to control human infections caused by *Candida* and *Cryptococcus* species. Med Chem Res. 2018;27:1043-1049. doi:[10.1007/s00044-017-2126-0](https://doi.org/10.1007/s00044-017-2126-0)
53. Yan Q, Cao R, Yi W, Chen Z, Wen H, Ma L, Song H. Inhibitory effects of 5-benzylidene barbiturate derivatives on mushroom tyrosinase and their antibacterial activities. Eur J Med Chem. 2009;44:4235-4243. doi:[10.1016/j.ejmech.2009.05.023](https://doi.org/10.1016/j.ejmech.2009.05.023)
54. Egorova S, Ivanova VN, Putokhin NI. Thiophene aldehyde and its derivatives. Chem Heterocycl Comp. 1967;3:654. doi:[10.1007/BF00468337](https://doi.org/10.1007/BF00468337)
55. Ramesh G, Daravath S, Ganji N, Rambabu A, Venkateswarlu K. Facile synthesis, structural characterization, DNA binding, incision evaluation, antioxidant and antimicrobial activity studies of Cobalt(II), Nickel(II) and Copper(II) complexes of 3-amino-5-(4-fluorophenyl)isoxazole derivatives. J Mol Struct. 2019;1202:1-41. doi:[10.1016/j.molstruc.2019.127338](https://doi.org/10.1016/j.molstruc.2019.127338)
56. Ali I, Haque A, Saleem K, Hsieh MF. Curcumin-I Knoevenagel's condensates and their Schiff's bases as anti-cancer agents: synthesis, pharmacological and simulation studies. Bioorg Med Chem. 2013;21:3808-3820. doi:[10.1016/j.bmc.2013.04.018](https://doi.org/10.1016/j.bmc.2013.04.018)
57. Indumathy R, Kanthimathi M, Weyhermuller T, Nair BU. Cobalt complexes of terpyridine ligands: crystal structure and nuclease activity. Polyhedron 2008;27:3443-3450. doi:[10.1016/j.poly.2008.08.003](https://doi.org/10.1016/j.poly.2008.08.003)
58. Zhao P, Xu LC, Huang JW, Liu J, Yu HC, Zheng KC, Ji LN. Experimental and DFT studies on DNA binding and photocleavage of two cationic porphyrins: effects of the introduction of a carboxyphenyl into pyridiniumporphyrin. Spectrochim Acta A Mol Biomol Spectrosc. 2008;71:1216-1223. doi:[10.1016/j.saa.2008.03.031](https://doi.org/10.1016/j.saa.2008.03.031)
59. Hajian R, Ekhlasi E, Daneshvar R. Spectroscopic and electrochemical studies on the interaction of epirubicin with fish sperm DNA. J Chem. 2012;9:1587-1598. doi:[10.1155/2012/738678](https://doi.org/10.1155/2012/738678)
60. Campillos M, Kuhn M, Gavin AC, Jensen LJ, Bork P. Drug target identification using side-effect similarity. Science. 2008;321:263-266. doi:[10.1126/science.1158140](https://doi.org/10.1126/science.1158140)
61. Keiser MJ, Roth BL, Armbruster BN, Ernsberger P, Irwin JJ, Shoichet BK. Relating protein pharmacology by ligand chemistry. Nat Biotechnol. 2007;25:197-206. doi:[10.1038/nbt1284](https://doi.org/10.1038/nbt1284)
62. Ali A, Khalid M, Rehman MF, Haq S, Ali A, Tahir MN, Ashfaq M, Rasool F, Braga AAC. Efficient synthesis, SC-XRD, and theoretical studies of O-Benzene-sulfonylated pyrimidines: Role of noncovalent interaction influence in their supramolecular network. ACS Omega. 2020;5:15115-15128. doi:[10.1021/acsomega.0c00975](https://doi.org/10.1021/acsomega.0c00975)
63. Ooretir C, Kaniskan N. Frontier orbital theory and chemical reactivity: The utility of spectroscopy and molecular orbital calculations. Recent Experimental and Computational Advances in Molecular Spectroscopy. 1993:351-367.
64. Anup Pandith, Young Jun Seo. Label-free sensing platform for miRNA-146a based on chromofluorogenic pyrophosphate recognition. J Inorg Biochem. 2020;203:1-41. doi:[10.1016/j.jinorgbio.2019.110867](https://doi.org/10.1016/j.jinorgbio.2019.110867)
65. George J, Prasana JC, Muthu S, Kuruvilla TK, Savanthi S, Saji RS. Spectroscopic (FT-IR, FT-Raman) and Quantum mechanical study on N-(2,6 dimethyl phenyl)-2-{4-[2hydroxy-3-(2methoxyphenoxy)propyl]piperazin-1yl}acetamide. J Mol Struct. 2018;1171:268-278. doi:[10.1016/j.molstruc.2018.05.106](https://doi.org/10.1016/j.molstruc.2018.05.106)